

# Mathematical models for an undisturbed soil-column

Written by C. Sean Bohun\*

## Problem presented by:

Gongsheng Li (Shandong University of Technology)

## Problem Working Group:

C. Sean Bohun (University of Ontario Institute of Technology),

Huihui Dai (City University of Hong Kong),

Alistair Fitt (University of Southampton),

Huaxiong Huang (York University, Toronto),

Gongsheng Li (Shandong University of Technology),

Johnathan Wylie (City University of Hong Kong)

## 1 Introduction

Zibo is a prefecture-level city located in the central portion of Shandong province in the People's Republic of China. Some of the major industries of this region include the petrochemical, pharmaceutical, china and ceramics sectors. Zibo is also abundant in natural resources. In support of the ceramics industry, they have large reserves of clay, limestone and bauxite. Consequently, there are a number of mines in the region and the outflow of acidic water from these metal and coal mines, known as acid mine drainage (AMD), is considerable. The AMD is rich in  $\text{SO}_4^{2-}$  (sulphate) ions and contains other pollutants that are subsequently transferred to the soils and surrounding surface rivers through both irrigation and infiltration of the ground water.

To understand the behaviour of the soil in the presence of infiltrating pollutants and atmospheric precipitation, soil-column experiments were performed. A chosen soil sample was undisturbed in the sense that the structure of the soil layers and any pollutants within the column were preserved when the soil was transferred to the experimental apparatus. To simulate the processes that occur within the environment (infiltration and precipitation), polluted water (liquor) from a nearby source was introduced at the top of the column and once this material has infiltrated the column, clean water was allowed to flush through the apparatus. The initial concentration of various ions in the liquor were measured and throughout the experiment, the fluid that reaches the bottom of the column was collected and analysed.

The goal for the workshop is to derive a mathematical model that predicts the observed experimental time dependence of the ionic concentrations emerging from the bottom of the apparatus. Developing the model will require an understanding of the physical and chemical mechanisms of the solute transport through the soil. This is an important first step in the eventual development of remediation schemes for the contaminated soil.

## 2 Experimental Results

Figure 1 details the apparatus used to obtain the experimental data. To ensure that the flow rate into the column is constant, a pipe is used to remove the pressure head of the infiltrating fluids. In addition to this, a layer of silver sand (sand without contaminants) disperses the fluid uniformly across the cross sectional area of the column.

---

\*University of Ontario Institute of Technology. E-mail: sean.bohun@uoit.ca

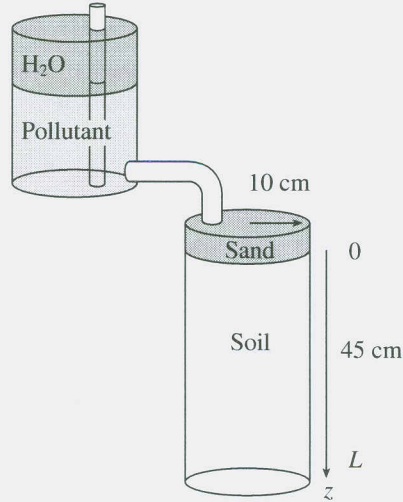


Figure 1: Schematic diagram of experimental apparatus.

Initially the ion concentration of various pollutants is measured in a fixed volume of 70300 ml and at  $t = 0$  this liquor is introduced at the top of the apparatus and allowed to percolate through the soil matrix. After  $t = 121$  hours the last of the pollutant enters the soil-column and a fixed volume of 21245 ml of clean water is allowed to flush through the apparatus. Throughout this process the concentration of the various ions in the fluid emerging from the bottom of the apparatus is recorded.

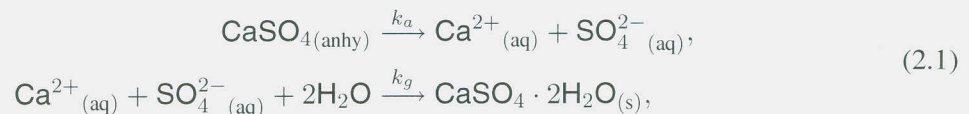
Since a fixed volume of 70300 ml passes through the soil matrix of a fixed radius of 10 cm over a period of 121 hours, an estimate of the bulk fluid flow rate through the column is simply the Darcy speed

$$q = \frac{\text{volume}}{\text{area} \cdot \text{time}} = \frac{70300 \text{ ml} \cdot 10^{-6} \text{ m}^3 \text{ ml}^{-1}}{\pi \cdot 10^{-2} \text{ m}^2 \cdot 121 \text{ hr} \cdot 3600 \text{ s hr}^{-1}} \sim 5.14 \times 10^{-6} \text{ m s}^{-1}.$$

Consequently the fluid takes about  $t = \tau = 24.3$  hours to propagate the complete length of the column,  $L = 45$  cm. Typical measured concentration profiles of various substances as a function of time are shown in Figure 2 and the corresponding data points can be found in the Appendix. On these plots time  $t$  is measured in units of  $\tau$  and the two dashed lines correspond to the onset of clean water, ( $t = 4.97\tau = 121$  hours), and the total infiltration time, ( $t = 6.64\tau = 161.5$  hours). The dashed-dot line is the initial concentration of the ionic species (i.e. the concentration in the liquor).

A few characteristics are immediately apparent. First, there is hardly any change in the concentration of the sodium  $\text{Na}^+$ , chlorine  $\text{Cl}^-$ , or bicarbonate  $\text{HCO}_3^-$  ions. This indicates that these ions simply propagate through the soil matrix without interacting. Which ion species can be ignored will depend on the contents of the soil being tested and may vary from one site to another. Second, though the potassium ion  $\text{K}^+$ , displays interesting behaviour, this ion only occurs in trace amounts compared to the other species. We will thus ignore its presence for purposes of this analysis.

This leaves the calcium  $\text{Ca}^{2+}$ , magnesium  $\text{Mg}^{2+}$ , and sulphate  $\text{SO}_4^{2-}$  ions. Their similar shape leads one to believe that these ions may be involved in similar reactions within the soil column. On consulting a basic inorganic chemistry text [4] we found two reactions involving these ions that could be occurring in the soil. These include i) the dissolution of anhydrous  $\text{CaSO}_4$  and the subsequent crystallization of  $\text{CaSO}_4 \cdot 2\text{H}_2\text{O}_{(s)}$  (gypsum - plaster):



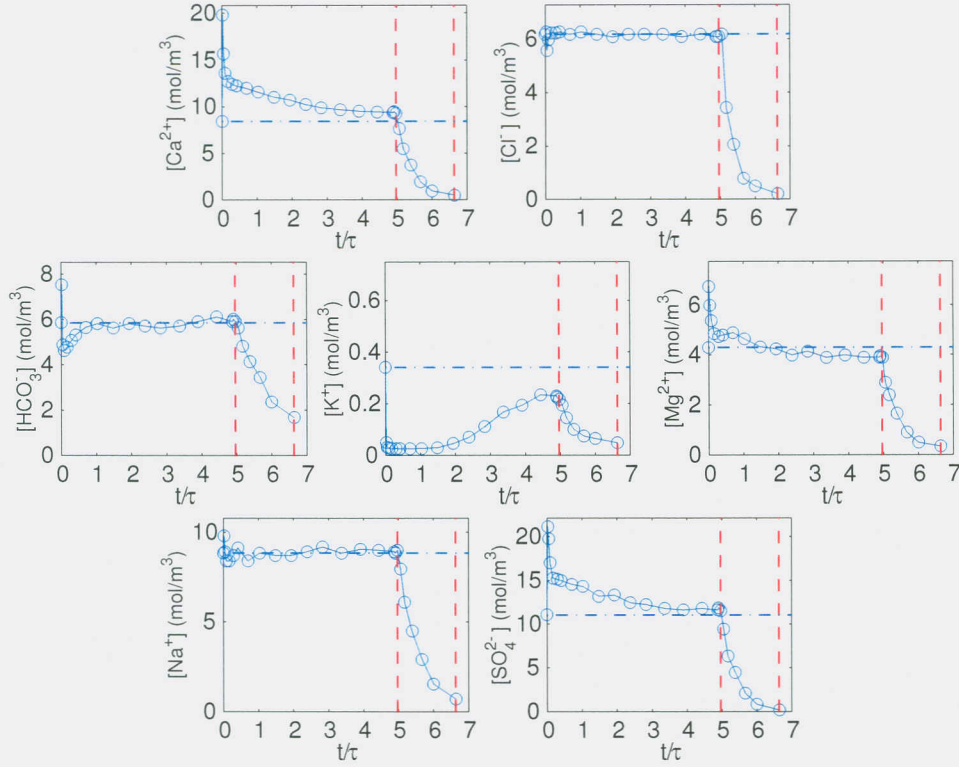
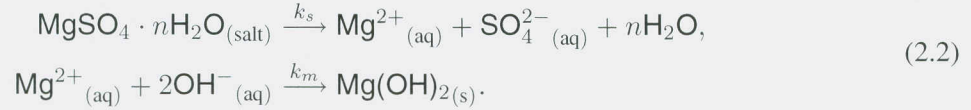


Figure 2: Experimental concentration curves for the seven pollutant ions under consideration. The vertical dashed lines correspond to the times of i) initial infiltration of clean water and ii) the total infiltration time. Initial concentrations of the various ionic species are indicated by the horizontal dashed-dotted lines.

and ii) the formation of insoluble  $\text{Mg}(\text{OH})_{2(s)}$  (“milk of magnesia”) from the dissolution of magnesium sulphate salts:



This last reaction is typically written as



but since the sodium ions remain aqueous throughout this reaction we have chosen to omit them. We assume that  $\text{OH}^{-}$  will always be available to this latter reaction since the measured soil acidity remains at  $\text{pH} = 7$ .

### 3 Mathematical Model

A number of assumptions have to be made before proceeding to develop a mathematical model. We start by assuming that there are no free ions in the soil, and that all of the ions propagate at the Darcy speed  $q = 5.14 \times 10^{-6} \text{ m s}^{-1}$ . The Péclet number  $\text{Pe} = \langle v \rangle d / D_m$  is a dimensionless constant which is useful to characterize the competition between diffusion and advection. In this case  $\langle v \rangle$  is the average fluid speed,  $d$  is a length scale dependent on the local geometry and  $D_m$  is the molecular diffusion constant. Considering (for example)  $\text{Cl}^{-}$  ions, with  $D_m = 1.5 \times 10^{-9} \text{ m}^2 \text{ s}^{-1}$  [5],  $\langle v \rangle = q$  and soil particles

with a diameter of  $d \sim 10^{-4}$  m we find  $Pe \sim 0.34 < 5$  so that the diffusion process dominates the spread of ions [9]. For larger values of the Péclet number advection dominates and one should replace the coefficient of molecular diffusion with a dispersion coefficient. Further discussion of the transition of the microscopic flow patterns as a function of  $Pe$  may be found in [10]. For simplicity we assume that the molecular diffusion constant  $D_m = 10^{-9} \text{ m}^2 \text{ s}^{-1}$  for all ions. These values are readily available in the literature [8, 13] and can be used to further refine the model.

If we assume that the reaction kinetics for the ion/salt reactions are governed by the law of mass action, and furthermore, given by simple first and second order reactions, then the rate of change of the various concentrations can be easily derived. For simplicity we assume that each of these reaction occurs only in one direction, but, if required, it would not be difficult to account for reversible reactions if one knew the solubility products of the various salts which are available in [7]. The effect of including these additional terms is analogous to the addition of carrying capacities in equations of population dynamics. We denote by  $\mathbf{s} = (s_1, s_2, s_3, s_4)^T$  the amounts of the four non-ionic compounds:  $\text{CaSO}_4(\text{anhy})$ ,  $\text{CaSO}_4 \cdot 2\text{H}_2\text{O}(\text{s})$ ,  $\text{MgSO}_4 \cdot n\text{H}_2\text{O}(\text{salt})$ , and  $\text{Mg}(\text{OH})_2(\text{s})$  and the concentration of the ionic species:  $[\text{Ca}^{2+}]$ ,  $[\text{SO}_4^{2-}]$ , and  $[\text{Mg}^{2+}]$  as  $\mathbf{c} = (c_1, c_2, c_3)^T$ . For those locations that are saturated with fluid the non-ionic compounds satisfy

$$\dot{s}_1 = -k_a s_1, \quad \dot{s}_2 = k_g c_1 c_2, \quad \dot{s}_3 = -k_s s_3, \quad \dot{s}_4 = k'_m c_3, \quad (3.1a)$$

where the dots denote differentiation with respect to time, and  $k'_m = k_m [\text{OH}^-]^2$  and  $[\text{OH}^-] = 1 \times 10^{-7} \text{ mol l}^{-1}$ . For the ion species,

$$\dot{\mathbf{c}} = \begin{pmatrix} k_a s_1 - k_g c_1 c_2 \\ k_a s_1 - k_g c_1 c_2 + k_s s_3 \\ k_s s_3 - k'_m c_3 \end{pmatrix}. \quad (3.1b)$$

In the soil column we have advection and diffusion coupled with these reactions. The simplest model is the advection-diffusion equation

$$\frac{\partial \mathbf{c}}{\partial t} + q \frac{\partial \mathbf{c}}{\partial z} = D_m \frac{\partial^2 \mathbf{c}}{\partial z^2} + \begin{pmatrix} k_a s_1(z) e^{-k_a t} - k_g c_1 c_2 \\ k_a s_1(z) e^{-k_a t} - k_g c_1 c_2 + k_s s_3(z) e^{-k_s t} \\ k_s s_3(z) e^{-k_s t} - k'_m c_3 \end{pmatrix}, \quad (3.2a)$$

on the domain  $t > 0, 0 < z < \zeta, \zeta = \min\{qt, L\}$ . In this expression  $s_1$  and  $s_3$  have been solved in terms of their initial distributions within the column. For the soil, we assume that initially there are no free ions and furthermore, that ions can only arise from the infiltrating pollutant or the dissolution of salts which are embedded within the soil matrix. This gives the initial condition

$$\mathbf{c}(z, 0) = \mathbf{0}, \quad 0 < z < L. \quad (3.2b)$$

Ions leave the soil-column with no velocity so we impose a no flux condition at  $z = L$ . At the top of the soil-column,  $z = 0$ , the pollutant is applied for  $0 < t < T_f$  ( $T_f = 121$  hours) at which point the column is flushed with clean water. Our boundary conditions are therefore

$$\mathbf{c}(0, t) = \mathbf{c}_0 H(T_f - t), \quad t > 0, \quad (3.2c)$$

$$\frac{\partial \mathbf{c}}{\partial z}(L, t) = \mathbf{0}, \quad t > 0 \quad (3.2d)$$

where  $H$  is the Heaviside unit step function.

Expression (3.2) describes the concentration profiles of the three ionic species and gives rise to six unknowns: the four reaction rates  $k_a, k_g, k_s, k'_m$  and the initial salt distributions  $s_1(z)$  and  $s_3(z)$ .

### 3.1 Non-dimensionalization

Identification of sets of parameters that characterize the behaviour can most easily be found by rescaling the variables. We rescale length and time using the length of the column and the Darcy speed respectively so that

$$z = L\hat{z}, \quad t = \frac{L}{q}\hat{t}, \quad \mathbf{s} = \Gamma\hat{\mathbf{s}}, \quad \mathbf{c} = \Gamma\hat{\mathbf{c}}.$$

with  $\Gamma = 10 \text{ mol m}^{-3}$ , a characteristic concentration. Here variables with hats ( $\hat{\cdot}$ ) are the non-dimensional ones. Letting  $\epsilon = D_m/qL = 4.33 \times 10^{-4}$ ,  $T = qT_f/L = 4.97$  and denoting

$$k_1 = \frac{k_a L}{q}, \quad k_2 = \frac{k_g L \Gamma}{q}, \quad k_3 = \frac{k_s L}{q}, \quad k_4 = \frac{k'_m L}{q},$$

the diffusion equation (3.2a) becomes (after dropping hats)

$$\frac{\partial \mathbf{c}}{\partial t} + \frac{\partial \mathbf{c}}{\partial z} = \epsilon \frac{\partial^2 \mathbf{c}}{\partial z^2} + F(\mathbf{s}, \mathbf{c}, t), \quad 0 < z < \min\{t, 1\}, \quad t > 0, \quad (3.3a)$$

where

$$F(\mathbf{s}, \mathbf{c}, t) = \begin{pmatrix} k_1 s_1(z) e^{-k_1 t} - k_2 c_1 c_2 \\ k_1 s_1(z) e^{-k_1 t} - k_2 c_1 c_2 + k_3 s_3(z) e^{-k_3 t} \\ k_3 s_3(z) e^{-k_3 t} - k_4 c_3 \end{pmatrix}. \quad (3.3b)$$

The boundary and initial conditions (3.2b)-(3.2d) become

$$\mathbf{c}(z, 0) = \mathbf{0}, \quad 0 < z < 1, \quad (3.3c)$$

$$\mathbf{c}(0, t) = \mathbf{c}_0 H(T - t), \quad t > 0, \quad (3.3d)$$

$$\frac{\partial \mathbf{c}}{\partial z}(1, t) = \mathbf{0}, \quad t > 0. \quad (3.3e)$$

## 4 Parameter Estimation

The values of  $k_a$  and  $k_g$  in (2.1) can be estimated by performing an experiment on this system in isolation. In this case, experimental data is available for the in situ monitoring of the amounts of  $\text{CaSO}_4(\text{anhy})$  and  $\text{CaSO}_4 \cdot 2\text{H}_2\text{O}(\text{s})$  [15].

Returning to dimensional variables, and letting  $\mathbf{u} = (s_1, s_2, c_1, c_2)^T$ , the set of equations describing this experiment are

$$\frac{d\mathbf{u}}{dt} = \mathcal{L}(\mathbf{u}, k_a, k_g) = \begin{pmatrix} -k_a s_1, \\ k_g c_1 c_2, \\ k_a s_1 - k_g c_1 c_2 \\ k_a s_1 - k_g c_1 c_2 \end{pmatrix}. \quad (4.1)$$

In this experiment 100% of  $\text{CaSO}_4(\text{anhy})$  powder (corresponding to a saturated  $\text{CaSO}_4$  solution of concentration  $17.63 \text{ mol m}^{-3}$ ) is loaded into a wet-cell device and the percent by weight of the amounts of  $\text{CaSO}_4(\text{anhy})$  and  $\text{CaSO}_4 \cdot 2\text{H}_2\text{O}(\text{s})$  are given as functions of time  $s_1^{\text{exp}}(t)$  and  $s_2^{\text{exp}}(t)$  respectively.

Estimation of  $k_a$  and  $k_g$  is given by solution of the minimization problem

$$\min_{k_a > 0, k_g > 0} (\|s_1 - s_1^{\text{exp}}\|_{l_2} + \|s_2 - s_2^{\text{exp}}\|_{l_2}), \quad (4.2)$$

$$\frac{d\mathbf{u}}{dt} = \mathcal{L}(\mathbf{u}, k_a, k_g), \quad \mathbf{u}(0) = (1, 0, 0, 0)^T.$$

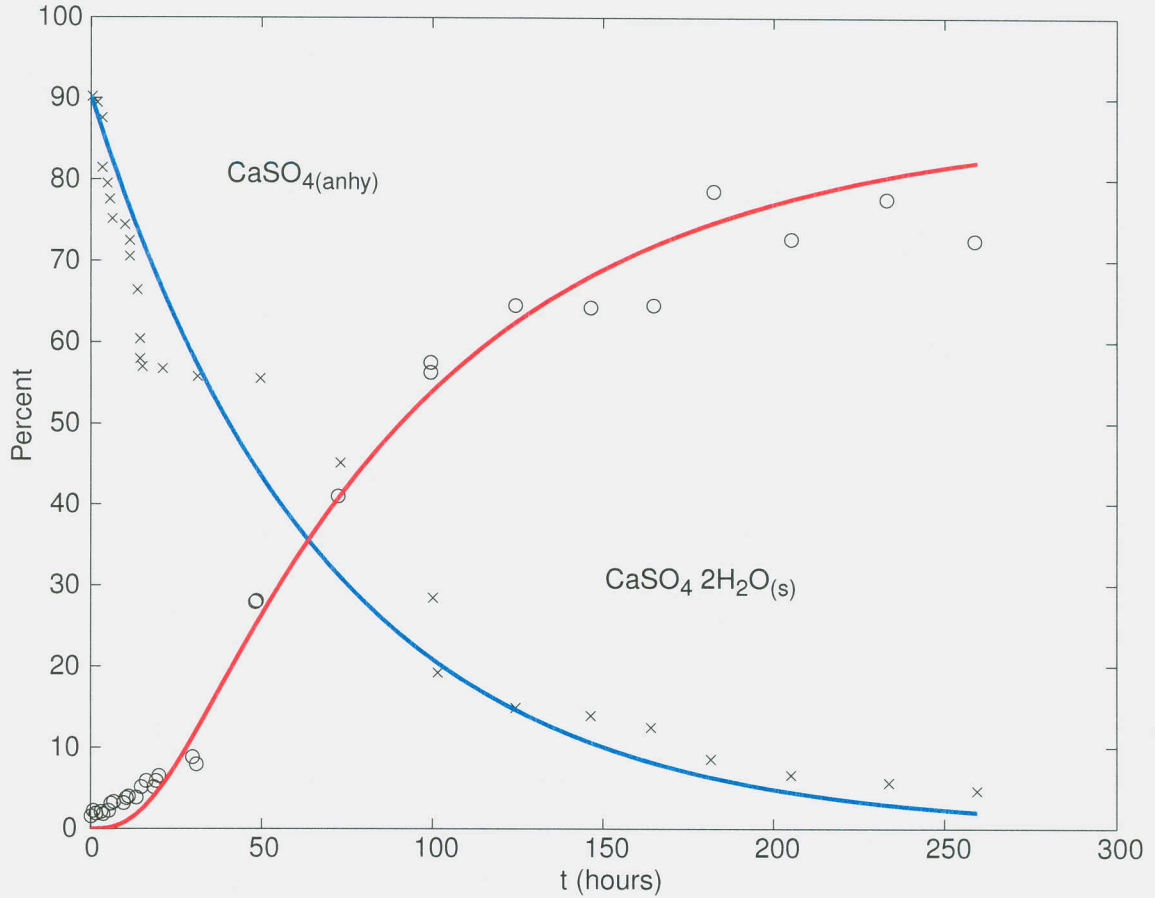


Figure 3: Experimental data from [15] and the best fit curves corresponding to  $k_a = 1.4622 \times 10^{-2} \text{ hr}^{-1}$ ,  $k_g = 1.720 \times 10^{-3} \text{ hr}^{-1}$  per percent.

Figure 3 reproduces the data points in [15] and solution curves of (4.2) with  $k_a = 1.4622 \times 10^{-2} \text{ hr}^{-1}$ ,  $k_g = 1.720 \times 10^{-3} \text{ hr}^{-1}$  per percent corresponding to  $k_1 = 0.3558$  and  $k_2 = 2.374$ .

In contrast to the gypsum reaction, the dissolution of magnesium salts to form  $\text{Mg}(\text{OH})_2$  is quite rapid. For the initial simulations we will therefore assume that  $k_3 = k_4 = 2$ .

## 5 Results & Discussion

Using the parameter set discussed above:  $k_1 = 0.3558$ ,  $k_2 = 2.374$ ,  $k_3 = 2$ ,  $k_4 = 2$ ,  $\epsilon = 4.33 \times 10^{-4}$ ,  $s_1(z) = s_3(z) = 0.5$ , the system (3.3) provided the break-through concentration shown in Figure 4. Also included is the applied pollutant concentration  $c_i(0, t)$  and the scaled experimental data from Figure 2.

For each of the curves there are three distinctive regions: an initial peak, a plateau region and a decay to zero. The peak is a result of the initial dissolution of salts and depends to a large extent on the values of  $k_1$  and  $k_3$  provided  $s_1(z)$  and  $s_3(z)$  are sufficiently large. The plateau region corresponds to time independent spatial distributions being set up in the soil. Ignoring diffusion, these time independent

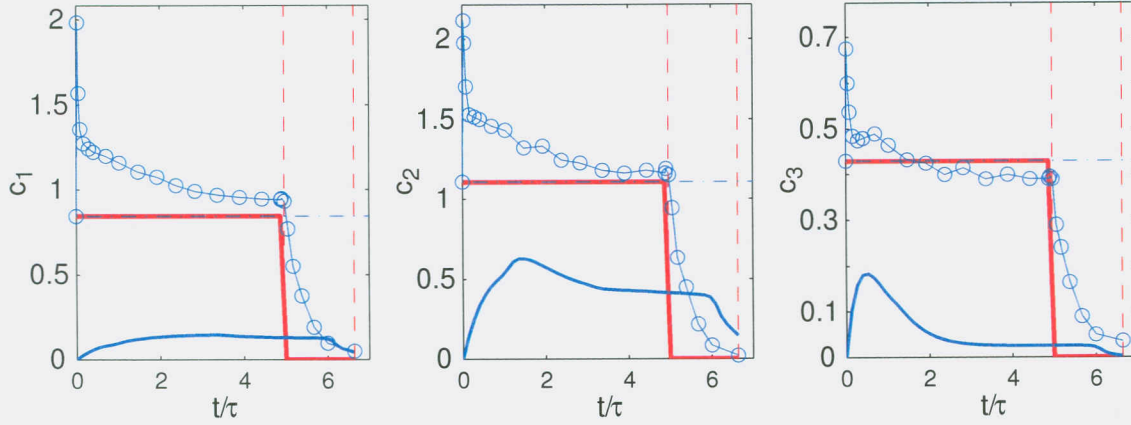


Figure 4: The break-through concentration,  $c_i(1, t)$ , applied concentration,  $c_i(0, t)$ , and experimental data for  $c_1 = [\text{Ca}^{2+}]$ ,  $c_2 = [\text{SO}_4^{2-}]$ , and  $c_3 = [\text{Mg}^{2+}]$ . For this simulation  $k_1 = 0.3558$ ,  $k_2 = 2.374$ ,  $k_3 = 2$ ,  $k_4 = 2$ ,  $\epsilon = 4.33 \times 10^{-4}$ ,  $s_1(z) = s_3(z) = 0.5$ .

profiles,  $c_{i,\text{eq}}(z) = \lim_{t \rightarrow \infty} c_i(z, t)$ , satisfy the initial value problem

$$\frac{d\mathbf{c}_{\text{eq}}}{dz} = - \begin{pmatrix} k_2 c_{1,\text{eq}} c_{2,\text{eq}} \\ k_2 c_{1,\text{eq}} c_{2,\text{eq}} \\ k_4 c_{3,\text{eq}} \end{pmatrix} = 0, \quad \mathbf{c}_{\text{eq}}(0) = \mathbf{c}_0 \quad (5.1a)$$

with solution

$$\mathbf{c}_{\text{eq}}(z) = \begin{pmatrix} \frac{c_{0,1}(c_{0,1}-c_{0,2})e^{-(c_{0,1}-c_{0,2})k_4 z}}{c_{0,1}e^{-(c_{0,1}-c_{0,2})k_4 z} - c_{0,2}} \\ \frac{c_{0,2}(c_{0,1}-c_{0,2})}{c_{0,1}e^{-(c_{0,1}-c_{0,2})k_4 z} - c_{0,2}} \\ c_{0,3}e^{-k_4 z} \end{pmatrix}. \quad (5.1b)$$

Finally the decay is characterized by the value of  $\epsilon$ .

The tableau of images in Figure 5 shows the effect of changing the various reaction rates. The top row is reproduction of the break-through curves in Figure 4 and rows two through five show the effect of i) increasing  $k_1$ , ii) decreasing  $k_2$ , iii) increasing  $k_3$ , and iv) decreasing  $k_4$  all by a factor of 10 respectively. Increasing  $k_1$  enhances the initial spike in  $c_1$  and  $c_2$ , while decreasing  $k_2$  increases the plateau value of these curves. The spike and plateau values of  $c_3$  are similarly controlled by  $k_3$  and  $k_4$ . Initial distributions of the salt,  $s_1(z)$  and  $s_3(z)$  primarily effect the break-through curves in the initial time period  $0 < t < 1$ . Material near the bottom of the column remains highly resolved as it leaves the column, whereas material near the top of the column is diffused across this time period.

The fact that the measured concentration at the bottom of the soil-column tracks the incident concentration without any delay suggests that some mechanism that has not been modelled is playing a significant role. Despite this, the model described in this report can quite successfully reproduce the experimental curves. Modifying the parameters to  $k_1 = 0.3558$ ,  $k_2 = 0.198$ ,  $k_3 = 1$ ,  $k_4 = 0.07$ ,  $\epsilon = 4.33 \times 10^{-4}$ ,  $s_1(z) = 1.1$ ,  $s_3(z) = 0.25$  and using  $c_{0,1} = 1.3$ ,  $c_{0,2} = 1.5$  produces the result in Figure 6.

One of the basic assumptions of our model is the applicability of an advection-diffusion equation. Anomalous flow has been observed elsewhere when the flow was intermittently stopped [14]. Combining a constant dispersion diffusion equation with a simple compartment model consisting of mobile, immobile, and excluded flows was shown to be sufficient to model the anomalous break-through curves. Even very recently, various compartment models have met with some success [1, 6, 16].

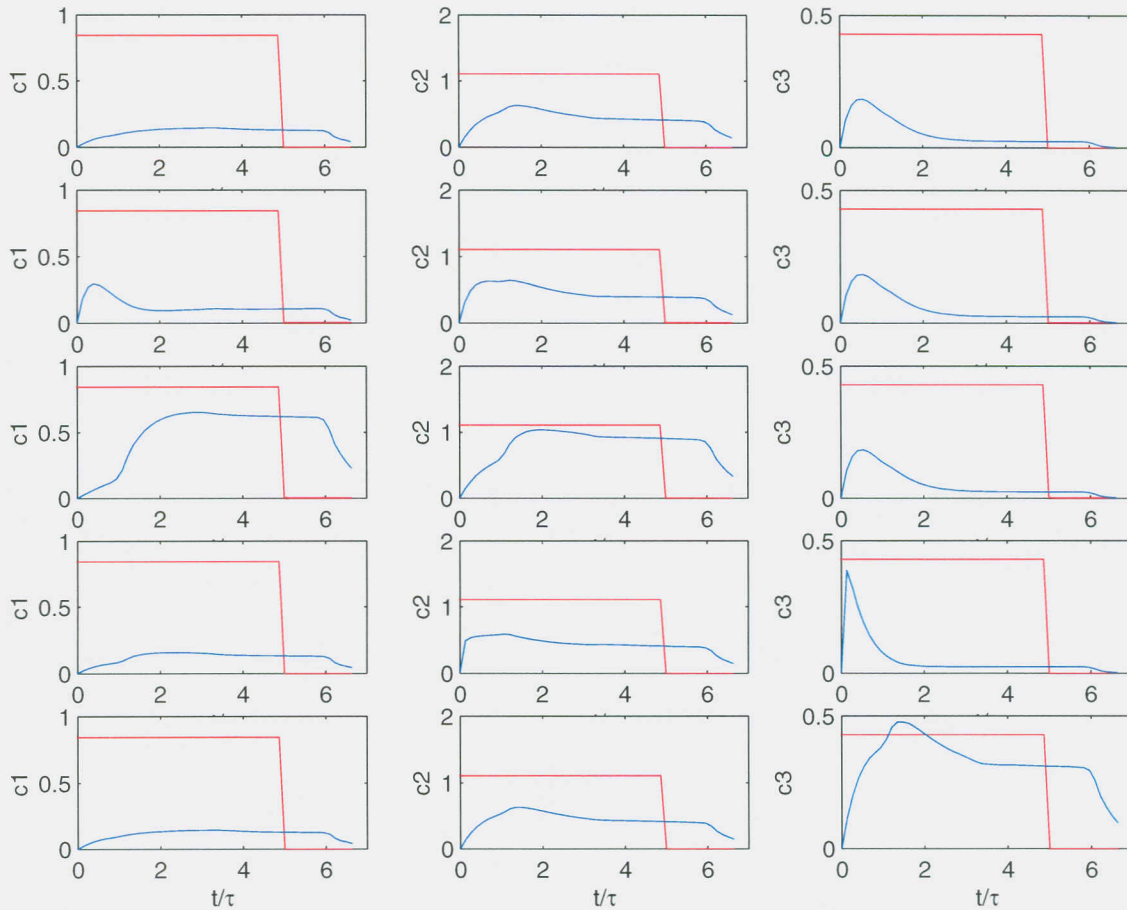


Figure 5: The effect of the reaction rates on the break-through concentration curves. The top row is the data from Figure 4 and is included for reference. Subsequent rows show the effect of i)  $k_1 \rightarrow 10k_1$ , ii)  $k_2 \rightarrow k_2/10$ , iii)  $k_3 \rightarrow 10k_3$ , and iv)  $k_4 \rightarrow k_4/10$ .

Since the soil-column is undisturbed, some attempt should be made to model the actual structures within the soil. Anomalous early arrival times and late time tailing in the break-through curves have been successfully modelled with a continuous time random walk (CTRW) theory [3]. This model is designed to retain the correlations of particles as they are advected across fractures in the medium and includes the classical advection-diffusion equation as a special case. Development of this model can be found in [2].

## 6 Conclusions & Recommendations

The observed concentration dependencies were reproduced, however in the process of matching the data, the rates of many of the reactions had to be significantly slowed. There is enough freedom in the model to produce quite complicated concentration profiles in the available parameter space so to eliminate some of this freedom, some effort should be made towards ensuring that the reactions proposed in this report are actually occurring within the soil-column. For the gypsum reaction, some older works [11, 12] may be useful to refine the model in this direction. With respect to the  $\text{MgSO}_4 \cdot n\text{H}_2\text{O}_{(\text{salt})}$  system, the reaction rates need to be determined. Finally, some effort should be made to account for structures within the undisturbed soil-column. The fact that compartment models have met with some success is not surprising

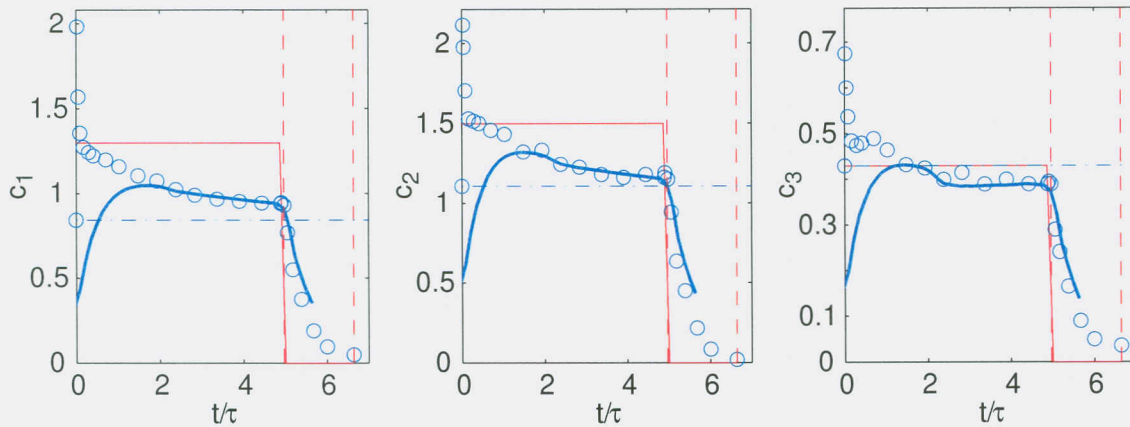


Figure 6: The break-through concentration,  $c_i(1, t)$ , and experimental data for  $c_1 = [\text{Ca}^{2+}]$ ,  $c_2 = [\text{SO}_4^{2-}]$ , and  $c_3 = [\text{Mg}^{2+}]$ . For this simulation  $k_1 = 0.3558$ ,  $k_2 = 0.198$ ,  $k_3 = 1$ ,  $k_4 = 0.07$ ,  $\epsilon = 4.33 \times 10^{-4}$ ,  $s_1(z) = 1.1$ ,  $s_3(z) = 0.25$ . Also,  $c_{0,1} = 1.3$ ,  $c_{0,3} = 1.5$  and the curves are shifted one unit to the left to align the onset of clean water flushing.

since these model typically add parameters that can be tuned to match experimental data. Development of a model that accounts for the wetting front and the initiation of the chemical reactions would be more ambitious but would significantly increase the understanding of the underlying processes.

## 7 Acknowledgements

The author would like to acknowledge City University of Hong Kong and the Lie Bie Ju Centre for Mathematical Sciences for their hospitality in hosting this event. A special thank you is reserved for Dr. Benny Hon and Dr. Huihui Dai. Their patience, hard work, and dedication ensured the success of the workshop.

## References

- [1] Alletto, L., Coquet, Y., Vachier, P. & Labat, C. (2006). Hydraulic conductivity, immobile water content, and exchange coefficient in three soil profiles. *Soil Science Society of America Journal*, **70**(4), pp. 1272-1280.
- [2] Berkowitz, B. & Scher, H. (1998). Theory of anomalous chemical transport in random fracture networks. *Physical Review E*, **57**(5), pp. 5858-5869.
- [3] Cortis, A. & Berkowitz, B. (2004). Anomalous transport in “classical” soil and sand columns. *Soil Science Society of America Journal*, **68**(5), pp. 1539-1548.
- [4] Cotton, F.A., Wilkinson, G. & Gaus, P.L. (1987). *Basic Inorganic Chemistry*. 2nd ed. John Wiley and Sons: New York.
- [5] Jalota, S.K. & Ghuman, B.S. (1992). Chloride movement in aggregated silt loam soil columns. *Soil Technology*, **5**, pp. 135-141.
- [6] Kim, Y-J., Darnault, C.J.G., Bailey, N.O., Parlange, J-Y. & Steenhaus, T.S. (2005). Equation for Describing Solute Transport in Field Soils with Preferential Flow Paths. *Soil Science Society of America Journal*, **69**(2), pp. 291-300.

- [7] Langmuir, D. & Melchior, D. (1985). The geochemistry of Ca, Sr, Ba and Ra sulfates in some deep brines from the Palo-Duro Basin, Texas. *Geochimica et Cosmochimica Acta*, **49**, pp. 2423-2432.
- [8] Li, Y-H & Gregory, S. (1974). Diffusion of ions in sea water and in deep-sea sediments. *Geochimica et Cosmochimica Acta*, **38**, pp. 703-714.
- [9] Lowe, C.P. & Frenkel, D. (1996). Do hydrodynamic dispersion coefficients exist? *Physical Review Letters*, **77**(22), pp. 4552-4555.
- [10] Martys, N.S. (1994). Fractal growth in hydrodynamic dispersion through random porous medium. *Physical Review E*, **50**(1), pp. 335-342.
- [11] Ostroff, A.G. (1964). Conversion of gypsum to anhydrite in aqueous salt solutions. *Geochimica et Cosmochimica Acta*, **23**, pp. 1363-1372.
- [12] Packter, A. (1974). Precipitation of calcium sulfate dihydrate from aqueous solution - induction periods, crystal numbers and final size. *Journal of Crystal Growth*, **21**, pp. 191-194.
- [13] Turnbull, A. & Ferriss, D.H. (1986). Mathematical modelling of the electrochemistry in corrosion fatigue cracks in structural steel cathodically protected in sea water. *Corrosion Science*, **26**(8), pp. 601-628.
- [14] Vogeler, I., Scotter, D.R., Clothier, B.E. & Tillman, R.W. (1998). Anion transport through intact soil columns during intermittent unsaturated flow. *Soil & Tillage Research*, **45**, pp. 147-160.
- [15] Warr, L.N. & Hofmann, H. (2003). In situ monitoring of powder reactions in percolating solution by wet-cell X-ray diffraction techniques. *Journal of Applied Crystallography*, **36**, pp. 948-949.
- [16] Zhang, H. & Selim, H.M. (2006). Modeling the transport and retention of arsenic (V) in Soils. *Soil Science Society of America Journal*, **70**(5), pp. 1677-1687.

Table 1: Raw soil-column data. Onset of clean water is at 121 hours.  
Concentration of ion species (mg/l)

$t$ (hr)	$\text{Ca}^{2+}$	$\text{Mg}^{2+}$	$\text{Na}^+$	$\text{K}^+$	$\text{HCO}_3^-$	$\text{SO}_4^{2-}$	$\text{Cl}^-$
0	338.28	104.42	203	13.36	357.56	1062.90	219.10
0.5	794.79	163.98	225	1.95	460.07	2031.67	222.29
1.1	628.65	145.75	205	1.25	297.76	1899.11	198.18
2.1	544.49	130.56	193	1.09	282.51	1637.82	212.01
4.1	510.42	117.79	193	1	291.66	1468.76	220.87
7.1	498.60	115.36	200	1.06	309.36	1454.35	220.87
10	490.60	116.58	210	1.04	324.61	1439.94	222.29
17	480.56	119.01	193	1.04	345.36	1401.04	219.10
25	464.53	112.93	203	1.06	354.51	1374.62	222.29
36	442.48	105.03	200	1.2	342.92	1268.47	219.10
47	430.46	103.20	200	1.81	354.51	1280.48	215.54
58	410.42	97.13	205	2.76	348.41	1195.95	219.08
69	396.39	100.77	211	4.35	342.92	1176.74	219.08
82	388.38	94.70	203	6.57	348.41	1133.03	219.08
95	382.36	97.13	208	7.58	360.61	1116.22	215.54
108	378.36	94.70	207	9.17	372.81	1133.03	219.08
119	376.35	94.70	205	9.01	360.61	1116.22	215.54
119.5	380.36	95.91	203	8.72	366.71	1142.63	215.54
121	372.34	94.70	207	8.49	360.61	1106.61	215.54
123	308.22	70.38	183	7.58	342.92	905.85	219.10
126	220.24	58.35	140	5.73	294.71	611.42	121.6
131	150.10	40.11	103	3.96	252.61	431.79	73.03
138	76.15	21.88	67	2.94	210.51	206.53	27.65
146	38.08	12.16	35.5	2.56	144	81.65	17.37
161.5	20.04	8.51	16.3	1.9	101.9	19.21	7.09